Structure Properties of Gallic Acid-Enhanced Alginate Hydrogels for Sustainable Food Packaging as Plastic Replacement

FOOD FRONTIERS Open Access

RESEARCH ARTICLE OPEN ACCESS

Structure Properties of Gallic Acid-Enhanced Alginate Hydrogels for Sustainable Food Packaging as Plastic Replacement

Francisco Javier Leyva-Jiménez[1,2] | Carlos Abellán-Dieguez[1,3] | Rodrigo Oliver-Simancas[4] | Antonio M. Rodríguez-García[1,5] | M. Elena Alañón[1,3]

[1]Regional Institute for Applied Scientific Research (IRICA), University of Castilla-La Mancha, Ciudad Real, Spain | [2]Area of Food Science and Technology, Faculty of Chemical Sciences and Technologies, University of Castilla-La Mancha, Ciudad Real, Spain | [3]Area of Food Science and Technology, Higher Technical School of Agronomic Engineering, University of Castilla-La Mancha, Ciudad Real, Spain | [4]Division of Industrial Biotechnology, Department of Life Sciences, Chalmers, University of Technology Kemivägen 10, Gothenburg, Sweden | [5]Area of Organic Chemistry, Faculty of Pharmacy, University of Castilla-La Mancha, Albacete, Spain

Correspondence: Antonio M. Rodríguez-García (antoniom.rodriguez@uclm.es) | M. Elena Alañón (mariaelena.alanon@uclm.es)

Received: 2 April 2025 | **Revised:** 2 June 2025 | **Accepted:** 11 June 2025

Funding: The study was supported by the project 2023-GRIN-34333, Programa FEDER Castilla-La Mancha and the project I+D+i PID2021-125188OA-C33 funded by MICIU/AEI/10.13039/501100011033, by ERDF, EU, A way of making Europe. It was also supported by the grant FJC2020-044298-I funded by MCIN/AEI/10.13039/501100011033 and by European Union NextGeneration EU/PRTR.

Keywords: alginate | antioxidant activity | food packaging | gallic acid | hydrogels | plastic replacement

ABSTRACT

Structure properties of alginate and glycerol hydrogels (93:7 v/v) functionalized with gallic acid (0.1%, 0.5%, and 0.8%) (w/v) were evaluated as plastic alternatives for food packaging. A thorough characterization of these hydrogels was performed, evaluating their physico-mechanical, optical, and functional properties, particularly for potential applications in food packaging. FTIR analysis confirmed interactions between the hydrogel matrix and gallic acid, highlighting the formation of hydrogen bonds. The BET method and high-resolution scanning electron microscopy (HRSEM) further verified the homogeneity of the hydrogel surfaces. The inclusion of gallic acid led to increased thickness, permeability, and swelling capacity. However, ultimate tensile strength and fracture toughness significantly decreased, especially in hydrogels containing the highest gallic acid concentration (0.8%). Functionalized hydrogels exhibited enhanced antioxidant activity, as demonstrated by DPPH and FRAP assays. Hydrogels with 0.5% gallic acid showed a 4.4–4.8-fold increase in antioxidant activity, while those with 0.8% gallic acid achieved a 7.0–7.3-fold enhancement. The release of gallic acid from the hydrogels followed a dose-dependent pattern, with peak release occurring within 1–2 h. These findings suggest that alginate-based hydrogels functionalized with gallic acid offer a promising approach for the controlled release of bioactive compounds, presenting potential applications in innovative packaging solutions.

1 | Introduction

The development of new materials built with natural components is one of the new challenges facing the scientific community as new environmental policies enacted by various international institutions aim to reduce environmental impact (European Commission 2020). Plastic continues to dominate food packaging due to its cost-effectiveness, durability, and versatility. However, grow-

ing global awareness of their environmental harm has spurred increased efforts to minimize its use. In line with the Sustainable Development Goals, the agri-food industry and scientific community are actively promoting sustainable practices in packaging. This includes exploring alternative materials that can effectively preserve food products while adopting a more environmentally friendly approach. In this context, hydrogels have been identified as promising materials for packaging applications due to their favorable physical and mechanical properties, including excellent moisture retention and flexibility, and potential biodegradability.

Hydrogels are a kind of advanced materials based on three-dimensional networks composed of hydrophobic polymers synthesized by crosslinking water-soluble polymers. Hydrogels can retain a large quantity of water within their network without disturbing their original structure (Smirnova and Gurikov 2018).

In this sense, hydrogels based on polysaccharides are a clear example of sustainable, green, non-toxic, and biocompatible components for novel materials. These natural polymers are characterized by abundant functional groups that enable them to be loaded with desired substances that can be released in a controlled manner over time (Coldebella et al. 2021; Niknia et al. 2020). The incorporation of active substances into polysaccharide-based hydrogels can be performed by several methods. For instance, the chemical grafting technique is used to covalently modify the structure of hydrogels, allowing the incorporation of specific functional groups (Feng et al. 2015). Hydrogels also can be modified using a layer-by-layer method that allows the construction of functional structures by alternating layers with different properties (Liu et al. 2018), or by vapor phase deposition allows the application of functional coatings on the surface of films (Dufour 2023). Among them, in situ, functionalization by wet impregnation is one of the most used methods in which gel constituents are in contact with the desired components for loading before or after the gelling process (Selvasekaran and Chidambaram 2021).

The wide variety of polysaccharides available makes possible the design of new tailor-made materials with customized properties. Particularly, alginate is a promising polysaccharide to produce functionalized materials (Choi et al. 2022). Alginate is a linear, anionic, and hydrophilic polysaccharide derived from marine algae, composed of mannuronic and guluronic acid units, and rich in carboxylic and hydroxyl functional groups (Leyva-Jiménez et al. 2023). However, to overcome the mechanical limitations of alginate-based materials, such as low elasticity and fragility, glycerol was added as a plasticizer to enhance the flexibility and mechanical properties of hydrogels, making them more suitable for various applications (Sun et al. 2018; Ye et al. 2023). In this manner, the carboxylic and hydroxyl groups present in both alginate and glycerol enhance their gelling ability with polyvalent metal ions. In addition, these functional groups also enhance the incorporation of bioactive compounds like polyphenols into the polymer network improving mechanical properties and providing antioxidant, antimicrobial, and controlled-release properties (Carbone et al. 2021; Fabra et al. 2018; Fernández-Ponce et al. 2021; Zhang et al. 2021). The weak interactions between the hydrogel matrix and phenolic compounds such as electrostatic interactions, hydrogen bonds or Van der Waals forces, enable sustained release and prolonged bioactivity (Lovskaya et al. 2015). Although their migration must comply with EU Regulation (EC) No. 1935/2004, phenolic compounds from natural sources are generally safe at proper concentrations (Siddiqui et al. 2023). Despite formulation challenges, many studies report the successful functionalization of biomaterials with polyphenols and assess their structure and release behavior (Harlen et al. 2025; Li et al. 2016; Yan et al. 2025).

Our hypothesis is that alginate films can be functionalized with pure gallic acid, a naturally abundant, simple phenolic compound with three hydroxyl groups, known for its proven antioxidant properties, to create new sustainable materials appropriate for food packaging as plastic replacement. The effects of varying concentrations of pure gallic acid (0.1%, 0.5%, and 0.8%) on the hydrogel's characteristics and properties were evaluated. A comprehensive characterization of gallic acid-functionalized alginate hydrogels was conducted including assessments of mechanical performances, water vapor permeability (WVP), swelling behavior, and surface structure via scanning electron microscopy (SEM). In addition, the hydrogels' loading capacity, antioxidant properties, and controlled release of gallic acid were analyzed, providing essential insights for designing their future applications in food packaging.

2 | Material and Methods

2.1 | Materials and Reagents

Sodium alginate was purchased from DuPont Nutrition As (Billingstad, Norway) with weight average molecular weight of 122 ± 15 KDa. The ratio of guluronic acid (G) to mannuronic acid (M) units in sodium alginate was 68/32 and the polydispersity index, the ratio of weight average molecular weight to number average molecular weight was 1.27 (data was provided by the manufacturer). On the other hand, glycerol, calcium chloride, and gallic acid (high purity grade $\geq$ 98.0%) were acquired from Sigma Aldrich (Steinheim, Germany). In addition, purified water was obtained by a Milli-Q system from Millipore (Bedford, MA, USA). For total phenolic content and antioxidant capacity determinations, methanol, Folin-Ciocalteu, sodium carbonate, DPPH: 2,2-Diphenyl-1-picrylhydrazyl radical, TPTZ: 2,4,6-tris(pyridin-2-yl)-1,3,5-triazine, ferric chloride, ferrous sulfate, sodium acetate, acetic acid, and hydrochloric acid were purchased from Sigma Aldrich (Steinheim, Germany). For the assessment of gallic acid release, sodium chloride, potassium chloride, sodium phosphate monobasic, and potassium phosphate dibasic were bought from Sigma Aldrich (Steinheim, Germany). All chemicals used were at least of reagent grade.

2.2 | Preparation of Alginate and Gallic Acid-Functionalized Alginate Hydrogels

For the preparation of hydrogels, a 1% (w/v) aqueous solution of sodium alginate was dissolved overnight at room temperature. After that, the alginate solution was mixed with glycerol at a ratio of 93:7 v/v and stirred until reached a homogeneous solution. With the aim of functionalizing alginate hydrogels, 0.1%, 0.5%, and 0.8% (w/v) of gallic acid was added and dissolved in the alginate-glycerol mixture. Then, 30 mL of these mixtures were

poured into plastic molds (20 × 10 × 1 cm) and gelled with a 0.2 M calcium chloride solution. For this purpose, 6 mL of calcium chloride solution (20% v/v) was sprayed on the surface of the mold and the gel formed was left to stabilize for about 20 min. After this, the hydrogel was dried overnight by forced air in a convection oven at 35°C until total loss of moisture. Finally, the films were removed and stored in a desiccator until further assays.

2.3 | Physicomechanical Characterization of Hydrogels

2.3.1 | Thickness

The thickness of the hydrogels was evaluated using a digital micrometer (0–25 mm ± 0.001) (Palmer Wahl, Asheville, NC, USA). The average thickening value of the films was determined by taking six measurements at random positions in the gel.

2.3.2 | Water Vapor Permeability

The WVP of alginate-based films was measured gravimetrically (ASTM E96/E96M-16 method) following the wet cup method, a standard test method for water transmission of materials (ASTM Committee 2016). Briefly, 10 mL of distilled water was placed in a VF2200-606 permeability cup (TQC Sheen, Molennbaan, Netherlands) with an inner diameter of 3.5 cm. Then, dried films were cut with a surface of 10 cm^2 and placed in the mouth of the cup. This system was closed and sealed with parafilm in order to warrant the passing of water vapor through the film. Finally, the cups were placed in a desiccator with silica gel keeping constant the temperature at 21 ± 1°C and ensuring a relative humidity of 0% inside the desiccator. In order to ensure reproducibility, the temperature was registered during the experiment. The moisture losses of the permeability cup were measured by weighing the cups each hour for 8 h. The WVP (g/kPa h m) was then determined using the following equations:

$$\mathrm{WVT} = \frac{\left(\frac{\Delta G}{t}\right) \times x}{A}, \tag{1}$$

where WVT was determined using the slope of weight loss in the permeability cup during the assay ($\Delta G/t$) and expressed as g/h. Moreover, the film thickness (x) in meters and the permeation area (A) in m^2 of the film were also used for determining the WVT which was expressed as g/h m.

$$\mathrm{WVP} = \frac{\mathrm{WVT}}{S \times (HR1 - HR2)}, \tag{2}$$

For determining the WVP, the saturation vapor pressure (S) at test temperature (21°C ± 1) in kPa (2.488 kPa at 21°C) and the difference humidity across both sides of the films inside the desiccator (HR1 = 0%) and inside the permeation cup (HR2 = 100%) were used. All experiments were performed in triplicate and the results are shown as an average and expressed in g/kPa h m.

2.3.3 | Mechanical Properties

Mechanical tests were carried out on a Mecmesin MultiTest-i 2.5-I dynamic mechanical analyzer (Mecmesin, West Sussex, UK) at room temperature. Tensile tests were carried out on hydrogels prepared on a mold made of Teflon, which meets the ISO 37 standard (ISO 37, 2024). Samples were anchored by tweezers on the analyzer and uniaxially stretched at 50 mm/min until their breaking point, using a cell load of 50 N. Ultimate Tensile Strength (UTS), Young's Modulus (YM), and Fracture Toughness (FT) were determined. Firstly, UTS was determined as the maximum pressure value supported by the hydrogel just before the break expressed in MPa. The Young´s modulus, which indicates the hydrogel elasticity, was calculated from the slope of the linear range of the stress–strain curve (between 2% and 10% of strain) and expressed as MPa. Finally, the critical stress intensity of a sharp crack where propagation of the crack suddenly becomes rapid and unlimited (FT), was determined from the area under the stress–strain curve in the linear range between 0% and 10% strain. FT was expressed as the energy absorbed by the gel in KJ/m^3. The experiments were performed at least in triplicate.

2.3.4 | Swelling Degree

Swelling studies were carried out by immersing the dried hydrogels cut into 1 cm diameter circles in Milli-Q water (pH = 7) at room temperature. The samples were weighed at established time intervals, finalizing the measurements when hydrogels had a constant weight. In order to avoid measurement errors by water weight, excess water was removed using a paper filter before each measure. The swelling degree was calculated by the following equation:

$$\text{Swelling Degree} = \frac{W_t - W_o}{W_o}, \tag{3}$$

where W_t is the weight of the hydrogels at each time and W_0 is weight of the dry hydrogel sample. All experiments were performed at least in triplicate and the results are expressed as weight gain in percentages of one.

2.3.5 | Brunauer–Emmett–Teller Experimental Setup

The total surface-area concentration and the amount of nitrogen gas required to condense a monolayer were measured experimentally using Brunauer–Emmett–Teller (BET) equipment through isotherms of adsorption and desorption and the distribution of the size of pores. These experiments were measured in a Gemini VII instrument (Micromeritics, GA, USA); Nitrogen gas was used as an adsorbate and the temperature at which the tests were performed was the temperature of liquid nitrogen (−195.79°C). For this test, the samples were degassed prior to the adsorption measurements.

2.3.6 | Scanning Electron Microscopy

The surface structure and morphology of the films were evaluated by high-resolution scanning electron microscopy (HRSEM)

using a Gemini SEM 500 (Zeiss, Germany). The analyses were performed on stable hydrogel samples that were lyophilized overnight after being frozen to avoid pressure disturbances during the measurement due to the release of water vapor that may be contained in the gel. The sample was observed under high vacuum conditions and an accelerated voltage of 3 kV. At least six micrographs were taken per film and those showing the typical surface morphology of each sample were selected.

2.3.7 | Thermogravimetric Analysis

To understand the thermal degradation during film storage, hydrogels were subjected to thermal stability assays. Thermogravimetric analysis was carried out in Q50 equipment (TA Instruments, DE, USA). The completely swollen hydrogels (10 mg) were frozen and lyophilized in a Telstar Lyoquest freeze dryer for 24 h (condenser temperature −80°C) (Telstar, Barcelona, Spain). The analysis was based on an isothermal under N_2 atmosphere at 100°C for 20 min and the following temperature ramp of 10°C each minute until it gets 800°C.

2.3.8 | Fourier Transform Infrared Analysis

The interaction among the components of the alginate-based films and the gallic acid was determined by an IR spectrometer which was recorded on FT-IR IRAffinity-1S equipment (Shimadzu Scientific Instruments, Japan) at room temperature. The infrared spectra of the film samples were taken between the wavelengths of 4000 to 400 cm^{-1} using a resolution of 4 cm^{-1}.

2.4 | Optical Characterization of Hydrogels

2.4.1 | Light Transparency and Opacity

The light transmittance of alginate-based hydrogels was evaluated at a wavelength of 600 nm using a UV-visible spectrometer (Helyos Gamma, Thermo, UK) with an empty test cell as the reference according to (Biao et al. 2019). All films were prepared, at least, in triplicate cutting 4 cm x 1 cm rectangles and placed in the outside face of the cell for each determination. Each sample was analyzed six times, and the results were shown as an average of the % of transmittance that passed through the gel. The opacity value was obtained using the same cut films and the value was expressed as a ratio between the absorbance value at 600 nm and the film thickness (mm).

2.4.2 | Colorimetric Measurements

The colorimetric assays were performed using a TR500 colorimeter (Lovibond, Hyderabad, India). The tristimulus color parameters were expressed according to CIELAB space color (CIE 1976 L^* a^* b^*). In this sense, lightness reflected the black ($L^* = 0$) or white (L^*100), redness ($a^* = +100$), or greenness ($a^* = -80$), and the yellowness ($b^* = +70$) or blueness ($b^* = -80$) of each film. In order to determine the total color difference between hydrogels (ΔE), the following formula was used:

$$\Delta E = \sqrt{(\Delta a*)^2 + (\Delta b*)^2 + (\Delta L*)^2}, \quad (4)$$

where Δa^*, Δb^*, ΔL^* are the differences between the color factors of the control film (alginate-glycerol-based hydrogel) and the hydrogels functionalized (0.1%, 0.5%, and 0.8% w/v) with gallic acid. Measurements were obtained at six points on each film, and the results were expressed as the mean of the results obtained.

2.5 | Functional Characterization of Hydrogels

2.5.1 | Total Phenolic Content

The total phenolic content of hydrogels was determined using the Folin–Ciocalteu colorimetric method according to Firoznezhad et al. (2023), with slight modifications. Firstly, the film extract was obtained by dissolving 0.1 g of hydrogel in 10 mL of methanol, keeping constant agitation at 200 rpm for 24 h. Each extraction procedure was performed in triplicate. Then, 10 μL of hydrogel extract, water (blank), or standard (calibration curve) was mixed with 600 μL of water and 50 μL of Folin–Ciocalteu's phenol reagent. After 10 min, 150 μL of sodium carbonate (20% w/v) and 190 μL of water were added to reach a final volume of 1 mL and kept in darkness for 2 h. After that, the absorbance was read at 760 nm against a blank in a Synergy H1 hybrid microreader (Biotek, Germany). A gallic acid calibration curve (5–150 μg/mL) was used in order to determine the amount of gallic acid incorporated in the gallic acid-functionalized alginate hydrogels. The total phenolic content was expressed as mg of gallic acid/g of hydrogel. All assays were done in triplicate.

2.5.2 | Antioxidant Properties

2.5.2.1 | DPPH Radical Scavenging Activity. The reduction of the radical DPPH was performed according to Leyva-Jiménez et al. (2023). Briefly, 10 μL of previous film extract or gallic acid solution (5–125 μg/mL) were dissolved in 990 μL of $DPPH^{\cdot}$ methanolic solution (40 μL/mL) and incubated in darkness and at room temperature. After that, the absorbance was evaluated at 517 nm, and the obtained results were expressed as mg of gallic acid/g of hydrogel. All experiments were performed in triplicate.

2.5.2.2 | Ferric Reducing Antioxidant Power Assay. The Ferric Reducing Antioxidant Power (FRAP) was carried out according to Benzie and Strain et al. (1996) with some modifications. A ferric complex of TPTZ (15.62 mg) and ferric chloride (16.22 mg) was mixed in 50 mL acetate buffer 0.3 M (pH 3.6). For these antioxidant assays, a $FeSO_4$ calibration curve (0.09–1.045 μM) was used. A 40 μL of hydrogel extract, blank solution (methanol), or standard solution was added to 250 μL of the previous ferric complex. After 4 min of incubation at 37°C in the dark, the absorbance was measured at 593 nm and results were expressed as the antioxidant capacity of mMol of $FeSO_4$ equivalents/g of hydrogel. All determinations were performed in triplicate.

2.5.3 | Release of Gallic Acid

The release of gallic acid by the hydrogels was indirectly assessed by the measurement of DPPH radical scavenging activity. For this purpose, 10 mg of each hydrogel was mixed with 1 mL of phosphate-buffered saline (PBS) at 37 ± 1°C. A 500 µL of the solution was collected at different times (0.25, 0.5, 1, 2, 4, 8, and 24 h) and kept in refrigeration until the assay described in Section 2.5.2.1. All experiments were developed in triplicate and the results were expressed in mg of gallic acid/g of hydrogel.

2.6 | Statistical Analysis

Data were handled by SPSS v.15. One-way analysis of variance (ANOVA) at a 95% confidence level ($p \leq 0.05$) was used to determine statistically significant differences among hydrogel parameters. Two post-hoc multiple comparison methods were employed depending on the result of the homogeneity of variances test of the results obtained: Tukey post-hoc analysis was used when the variances were homogeneous, otherwise, T3 Dunnet was applied to determine the statistical differences.

3 | Results and Discussion

3.1 | Physicomechanical Characterization of Hydrogels

Hydrogels derived from polysaccharides are known for their porous structure, low density, biocompatibility, and remarkable sustainable properties. However, the incorporation of other substances such as gallic acid, an antioxidant agent, can lead to changes in the structural properties of these macromolecular structures. In an exploration to understand the effects of different concentrations of gallic acid on the physical and mechanical properties of alginate hydrogels, a detailed comparative analysis was conducted. Table 1 provides an array of comparative metrics for the alginate hydrogel devoid of gallic acid with those functionalized with different concentrations of gallic acid. The evaluated properties included the thickness, WVP, swelling degree, UTS, YM, and FT.

3.1.1 | Thickness, WVP, and Swelling Degree

Evidence from our data and insights from various papers converge, illuminating a consistent positive correlation between the concentration of gallic acid and the increased thickness of alginate hydrogel films, a consensus echoed by other authors (Yan et al. 2025). The thickness increased from 92 ± 6 µm for the base film to 140 ± 4 µm for the film with 0.8% gallic acid, denoting a substantial thickening of approximately 52%.

Based on these results, it seems that gallic acid could be interacting with the alginate and glycerol, possibly leading to more cross-linking or layering within the material, which could account for the increased thickness. This fact was supported by Li et al. (2019), which discussed the fabrication of mechanically strong alginate/clay hydrogels and the effects of pH adjustment on their properties (Li et al. 2019). In addition, a higher water

TABLE 1 | Physicomechanical characterization of alginate and gallic acid-functionalized alginate hydrogels.

Hydrogels	Thickness (µm)	WVP × 10^{-5} (g/kPa h m)	Swelling Degree	UTS (MPa)	YM (MPa)	FT (KJ/m^3)	BET area (m^2/g)	Pore radius (nm)
Alg-Gly (93:7)	92 ± 6^{c}	1.97 ± 0.07^{c}	1.7 ± 0.6^{a}	2.2 ± 0.1^{a}	5.6 ± 0.5^{a}	732 ± 77^{a}	7.48	1.52
Alg-Gly (93:7), Gallic acid 0.1%	114 ± 7^{b}	3.4 ± 0.2^{b}	6.3 ± 1.0^{b}	1.9 ± 0.2^{a}	5.4 ± 0.7^{a}	$596 \pm 48^{a,b}$	6.01	1.53
Alg-Gly (93:7), Gallic acid 0.5%	114 ± 6^{b}	3.24 ± 0.02^{a}	4.7 ± 0.1^{b}	2.0 ± 0.3^{a}	5.5 ± 0.8^{a}	423 ± 27^{b}	7.29	1.71
Alg-Gly (93:7), Gallic acid 0.8%	140 ± 4^{a}	3.40 ± 0.08^{b}	5.0 ± 0.8^{b}	1.10 ± 0.02^{b}	5.3 ± 0.6^{a}	214 ± 64^{c}	13.83	1.72

Note: Values with different superscripts in the same column denote significant differences among aerogels according to the Tukey's post-hoc analysis ($p \leq 0.05$) when variances were homogenous, or according to T3 Dunnet post-hoc analysis ($p \leq 0.05$) for non-homogenous variances.
Abbreviations: Alg, Alginate; BET, Brunauer-Emmett-Teller method; FT, Fracture Toughness; Gly, Glycerol; UTS, Ultimate Tensile Strength; WVP, Water Vapor Permeability; YM, Young's Modulus.

adsorption rate, influenced by the presence of gallic acid, is also observed to contribute to this thickening effect. The augmented water-holding capacity facilitates a more pronounced swelling of the hydrogel films, compounding the effects of enhanced cross-linking and layering to result in a notable increase in thickness since larger gaps between polymeric chains remained after gel drying. This observation is in line with another study that indicates sodium alginate hydrogel is an appropriate material to load high amounts of phenolic acid compounds, such as gallic acid, showcasing its potential for increased thickness and water adsorption capacity (Santos et al. 2020). This observation aligns with findings reported in existing literature, both with gallic acid and similar compounds, further validating the correlation between gallic acid concentration and increased thickness of the alginate hydrogel films (Pereira et al. 2013; Yan et al. 2025).

This fact should be taken into account since thicker hydrogel film may offer better insulation properties due to its increased volume and more substantial structural integrity. Manzocco et al. (2021) underscored this by discussing the potential of hydrogels as novel packaging materials for food, emphasizing their low density and high porosity (Manzocco et al. 2021). However, it's essential to consider that thicker hydrogel might also lead to reduced flexibility, which could limit its applicability in flexible or dynamic environments. This is a crucial aspect to weigh when considering the balance between insulation and flexibility. In addition, an increase in thickness might also affect other hydrogel properties like permeability and transparency, an area that warrants further exploration to optimize the multifunctional utility of hydrogels in varied application scenarios (Batista et al. 2019; Selvasekaran and Chidambaram 2021; Zhou et al. 2021).

On the other hand, the alginate hydrogel developed exhibited a WVP of 1.97×10^{-5} g/kPa h m, significantly lower than that of comparable hydrogels reported in previously studies (3.4×10^{-4} and 2.88×10^{-4} g/kPa h m) indicating superior barrier properties (Biao et al. 2019; Choi et al. 2022). The incorporation of different percentages of gallic acid led to an increase in WVP, which is attributed to the presence of hydrophilic —OH groups in gallic acid. These groups enhance water uptake and swelling capacity, resulting in a more hydrated and expanded hydrogel network that facilitates the diffusion of water molecules (Table 1). This observation can be corroborated by the inherent mesoporosity of other hydrogels, as documented in prior studies (Barboza-Carmona et al. 2022). This hypothesis may explain the increased WVP permeability achieved by alginate hydrogel loaded with 0.8% w/v of gallic acid (3.4×10^{-5} g/kPa h m). This fact might be especially relevant in applications where moisture transmission is desirable, such as in some types of food packaging, where controlled permeability can help prevent condensation, reduce microbial growth, or even reduce the ethylene concentration, reducing the ripening of some fruits as apples or avocadoes.

The swelling degree is another property of hydrogels that should be considered. The incorporation of gallic acid into alginate-glycerol hydrogel led to a significant increase in swelling ratio values (Table 1) being 1.7 in the base film up to 6.5 in functionalized films with gallic acid. These results revealed that the obtained alginate hydrogels presented a swelling capacity within the range previously reported in the literature (Choi et al. 2022; Guan et al. 2024). This fact seemed to be attributable to the chemical structure of gallic acid whose hydroxyl groups can establish hydrogen bonds with water, leading to increased water uptake and swelling of the hydrogels. This interaction seemed to precipitate an increased water uptake and swelling of the alginate-based films, a phenomenon that had been corroborated by existing literature (Shivakumara and Demappa 2019). In the aforementioned study, the swelling behavior of sodium alginate/poly(vinyl alcohol) hydrogels was found to depend strongly on the concentration of glutaraldehyde and the pH of the surrounding environment. In contrast, our results showed that within the tested range of gallic acid concentrations (0.1%–0.8%), there were no significant differences in swelling degree, suggesting a possible threshold effect beyond which additional gallic acid does not further influence this property. Therefore, the hypothesis that gains more strength is related to the amount of hydroxyl groups provided by the gallic acid, thus causing an increase in the hydrogen bonds between gel and water, raising the swelling ratio of functionalized hydrogels compared to base hydrogel (Sharma et al. 2022).

3.1.2 | Mechanical Parameters

Another mechanical parameter assessed in the developed hydrogels was the UTS. The hydrogel non-functionalized exhibited an UTS of 2.2. MPa (Table 1). In this sense, the results were similar to those obtained by Chen et al. (2023) and Guan et al. (2024) who developed alginate composite hydrogels with gelatine and poly(vinyl alcohol), respectively (Chen et al. 2023; Guan et al. 2024). The addition of gallic acid at 0.1% and 0.5% did not evidence a significant change in the ability to resist tensile forces. However, the UTS value significantly drops to 1.10 MPa at the highest percentage of gallic acid tested (0.8%). This observation suggested that the incorporation of great concentrations of gallic acid might have compromised the tensile strength of the alginate hydrogels. Several papers support this observation, indicating that gallic acid may interfere with the cross-linking within the alginate–glycerol matrix, leading to reduced resistance to tensile forces (Giz et al. 2020; Zhan et al. 2015). Some authors found that the combination of glycerol, used as a plasticizer, and calcium crosslinking had a synergistic effect on the mechanical properties of alginate films (Giz et al. 2020). Other authors also observed changes in the physical properties of alginate films after cross-linking with calcium ions, supporting the idea that alterations in cross-linking can significantly affect the film's mechanical properties (Russo et al. 2007). Gallic acid might be introducing structural irregularities or disrupting intermolecular interactions within the hydrogel, as evidenced in the study by Zhan et al. (2015), which demonstrated the binding interaction between gallic acid and a carbohydrate structure, indicating the potential of gallic acid to interfere with other substances and networks, thereby weakening the overall structure and reducing the UTS (Zhan et al. 2015). However, this potential disadvantage must be evaluated in the context of the final application of these hydrogels. A lower tensile strength might not significantly impact the film's performance, especially if tensile forces are not a key consideration in the application. For instance, in applications like moisture absorption where tensile strength may not be the primary concern, the advantages of gallic acid incorporation might outweigh the decrease in UTS.

It is worthy to note, that the differential impact of gallic acid on the tensile strength and YM of alginate–glycerol hydrogels can be attributed to the complex interplay of molecular interactions and structural rearrangements induced by the acid. When gallic acid is incorporated, it may preferentially interact with specific components of the alginate–glycerol matrix, leading to a localized disruption in the network structure. This localized effect might cause a decrease in tensile strength as the structural integrity at certain points within the matrix is compromised. However, YM, a measure of the material's inherent elasticity, remains unaffected (Table 1) because it is largely dictated by the bulk properties of the material rather than localized structural alterations (Essifi et al. 2020). The macroscopic elastic behavior of the hydrogel encompasses a broader structural framework, rendering it less sensitive to localized disruptions caused by the introduction of gallic acid. The evaluation of mechanical properties, including the impact of gallic acid incorporation on YM, unveils insights into the nuanced behavior of the material. A constant YM (≈5.4 MPa) across different gallic acid concentrations implies that the material's inherent elastic properties are largely unaffected by the introduction of gallic acid. Our findings are supported by Essifi et al. (2020), who examined calcium alginate microbeads loaded with gallic acid and reported that, despite structural changes induced by the additive, the overall elasticity—as measured by YM—remained largely unaffected. Although their study did not vary gallic acid concentration, their observation of consistent elastic behavior under additive incorporation aligns with our results. This suggests that the inclusion of gallic acid while influencing other mechanical parameters such as tensile strength or WVP, does not compromise the elastic resilience of the hydrogel network. Essefi et al. further attributes this to delayed elasticity, likely resulting from a compensatory interplay between structural disruption and molecular interactions within the matrix (Essifi et al. 2020). The consistency of YM measurements with direct experimental findings underscores the resilience of the material's elastic properties, even amidst variations induced by gallic acid incorporation. Such consistency in stiffness despite variations in other properties may be advantageous for applications that require a stable response to deformation. According to the obtained results, the elasticity of alginate-based hydrogels obtained in this study was in line with values collected from the literature on alginate-based hydrogels (Bento et al. 2022) and quite higher than those developed with alginate without any plasticizer (Essifi et al. 2020).

On the other hand, the incorporation of gallic acid significantly reduced the FT (Table 1) which is a measure of resistance to fracture when a crack or other stress-concentrating defect is present. FT is indicative of a material's resistance to the propagation of cracks. When gallic acid was incorporated, it may interact with the polymeric chains and cross-linking bonds within the alginate–glycerol matrix in a manner that specifically affected the material's behavior under stress and its ability to resist crack propagation. The alginate hydrogel showed a toughness of 732 KJ/m^3 which was similar to those obtained by Guan et al. (2024). However, this parameter decreased with the concentration of gallic acid introduced, reaching a value of 214 KJ/m^3 for the hydrogel with the highest gallic acid loading. This substantial reduction implied that the addition of gallic acid made alginate–glycerol hydrogels more prone to fracture, suggesting a more brittle structure. This could be due to the gallic acid causing changes in the alginate–glycerol network, perhaps by disrupting the intermolecular bonds or introducing structural irregularities, which could promote crack propagation and thereby decrease the material's resistance to fracture. However, the reduction in FT might not necessarily limit the potential application of hydrogel since, in applications where the hydrogel would be exposed to minimal mechanical stress or where brittleness was not an important factor, this reduction in toughness might not be a disadvantage.

3.1.3 | Microstructure: Moisture Isotherm, Porosity, and HRSEM Observation

On the surface characterization and porosity of the alginate–glycerol materials, the BET method is commonly used for the characterization of the surface area of certain materials. These results provided essential insights into the structural characteristics of the alginate–glycerol and gallic acid-functionalized hydrogels (Table 1). It is important to note that the observed changes in pore radius across the different hydrogels did not exhibit a substantial variation, even with the gallic acid incorporation, where pore radius ranged from 1.52 to 1.72 nm. In addition, the surface area values were quite similar except for the hydrogel with 0.8% gallic acid, which showed the highest specific surface area (13.83 m^2/g). Although the surface area of these hydrogels was lower than similar alginate-based hydrogels previously reported (Martins et al. 2015; Viganó et al. 2020), these findings suggest that gallic acid alters the internal structure primarily by increasing surface complexity rather than significantly expanding pore dimensions. Previously, it had been reported that small changes in soft calcium concentration (20–25 mM) in calcium–alginate hydrogels did not induce changes in surface area, although the introduction of oxidized or peptide-grafted alginate in the gels resulted in larger pore sizes (Akbarzadeh Solbu et al. 2022). In the present study, while pore radius remained largely unchanged, the increased surface area with higher gallic acid content implies a rise in porosity or microstructural heterogeneity. This structural shift likely contributes to the mechanical behavior observed; greater porosity facilitates crack propagation, thereby reducing FT. This explanation is consistent with the lower UTS and increased WVP observed in functionalized hydrogels. The potential applications of these materials reside in the package of food which require certain permeability to gases such as ripening hormones, which can over-ripen when concentrated in small atmospheres such as a container (e.g. avocadoes or apples).

Despite these internal changes, HRSEM revealed homogeneous surface morphologies for both the control and gallic acid-loaded hydrogels (Figure 1), underscoring that microstructural differences may be more pronounced within the bulk than at the surface.

The lack of significant disparities in surface morphology may confirm the pore radius data since the values were similar in all the hydrogels tested. However, the SEM images did not explain the increase in surface area, since the resolution of the technique applied to the structural images obtained made it difficult to visualize pores with such a small size and, therefore, did not allow verification of these results. Further study of the hydrogels obtained by cryogenic fracture, particularly on the cross sections,

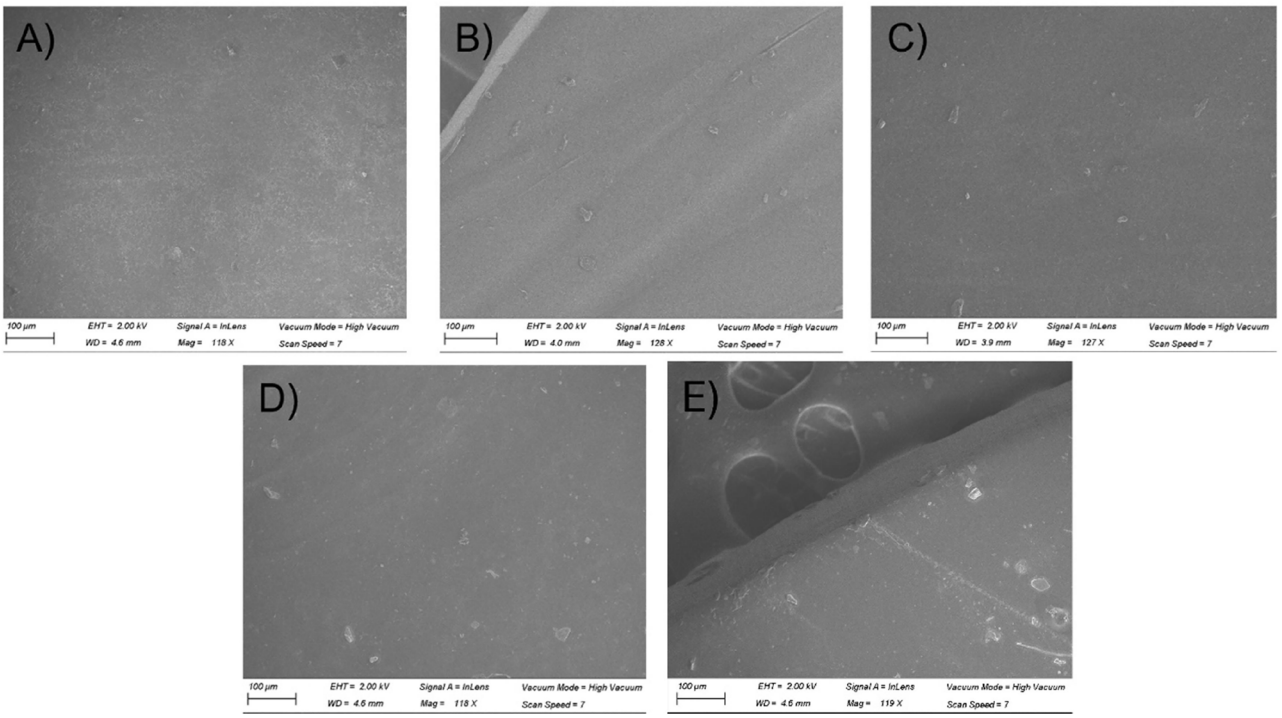

FIGURE 1 | HRSEM micrographs of alginate and gallic acid-functionalized alginate hydrogels: alginate–glycerol (93:7) (A); alginate–glycerol (93:7) with 0.1% of gallic acid (B); alginate–glycerol (93:7) with 0.5% of gallic acid (C); alginate–glycerol (93:7) with 0.8% of gallic acid (D) and its cross section (E).

provides more detailed insights into the microstructural features, and the homogeneity of the hydrogel matrix. Notably, in the hydrogels with the highest concentration of gallic acid (0.8%), the SEM images revealed the presence of gallic acid crystals forming within the structure (Figure 1E). These crystals are clearly visible and indicate a significant interaction between the gallic acid and the hydrogel matrix, particularly at higher concentrations. This crystallization could potentially impact the mechanical and functional properties of the hydrogels, providing a unique insight into the material's behavior and performance.

3.1.4 | Thermal Stability

On the other hand, an analysis of the thermal properties of impregnated alginate–glycerol hydrogels functionalized with gallic acid, is imperative to understand how these additives can influence material performance under varying temperature conditions. Upon investigating the thermal behavior of the impregnated alginate–glycerol hydrogel with gallic acid, it was evident that their profiles shared similarities with the raw alginate–glycerol (Figure 2).

However, there are some discernible differences. The initial mass loss in the curve (approximately at 150°C), was caused by moisture evaporation and the release of coordinated water. Due to the ability of the gallic acid-loaded film to hold more water, as can be seen from the swelling values previously shown, the drop is slightly more pronounced in the functionalized films. The second mass weight (between 200°C and 280°C) presented by all gels was indicative of alginate thermal decomposition and may be associated with the fracture of glycosidic bonds, dehydration, decarboxylation, and decarbonylation of alginate and release of CO_2 and H_2O. It should be noted that the second weight loss of the functionalized films occurred earlier and with a lower weight loss than the base film. Moreover, the weight loss was lower the higher the concentration of gallic acid loaded. This seems to indicate that the degradation of gallic acid, being a simple phenolic acid, occurs slightly earlier than that of alginate, and contributes to the total residual mass of the gel after processing. Similar observations on the thermal stability of alginate-based hydrogels were reported, reinforcing the findings presented (Y. Liu et al. 2016).

3.1.5 | FT-IR Spectra

Fourier Transform Infrared Spectroscopy (FTIR) was used to discern potential chemical interactions between gallic acid and the constituents of the alginate–glycerol hydrogels. The distinct FTIR spectra for alginate hydrogel and those loaded with gallic acid can be seen in Figure 3.

Thus, as can be seen in Figure 3, the FTIR spectrum of the alginate–glycerol hydrogel shows characteristic absorption bands corresponding to the functional groups of both components. A broad peak around 3200–3400 cm^{-1} is attributed to O—H stretching vibrations, indicating extensive hydrogen bonding from hydroxyl groups in alginate, glycerol, and possibly absorbed water (Jejurikar et al. 2012). The peak near 2900 cm^{-1} corresponds to the C—H stretching of aliphatic groups of glycerol. Key bands around 1595–1610 and 1410–1425 cm^{-1} are assigned to the asymmetric and symmetric stretching of carboxylate groups (COO^-) in alginate, which are crucial for assessing ionic interactions or

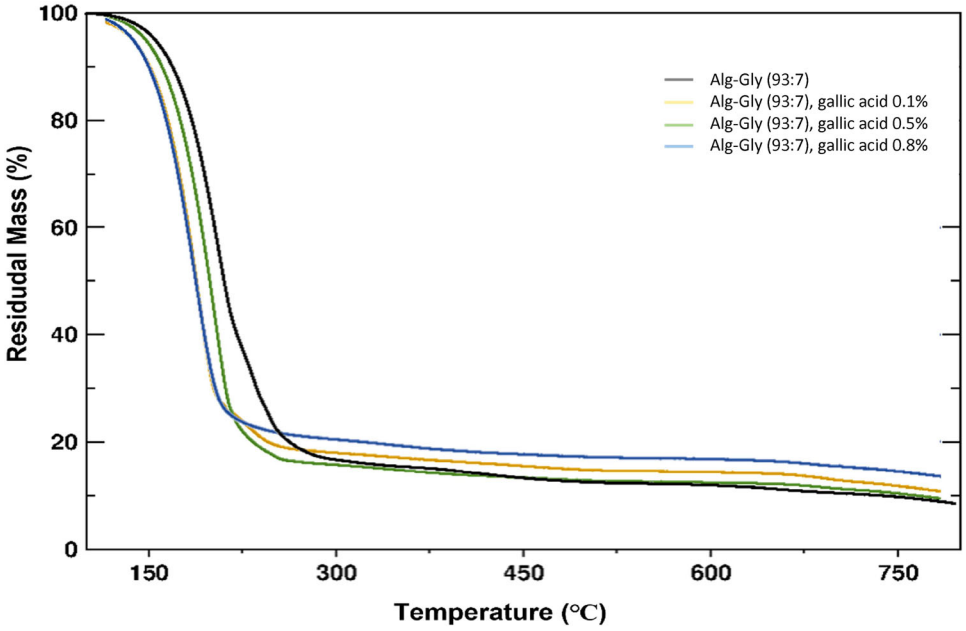

FIGURE 2 | Thermogravimetric analysis (TGA) of alginate and gallic acid-functionalized alginate aerogels in nitrogen atmosphere.

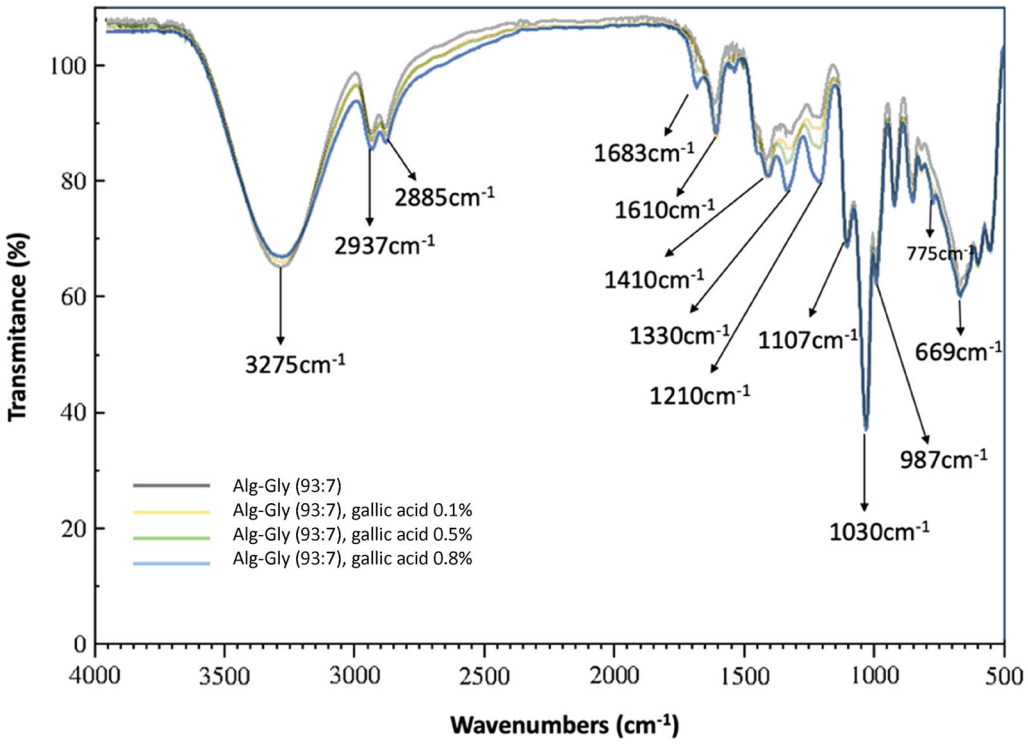

FIGURE 3 | FTIR spectrum of alginate and gallic acid-functionalized alginate hydrogels.

crosslinking (Pawar and Edgar 2012; Rinaudo 2008). The strong, complex signals between 1020 and 1080 cm^{-1} are associated with C—O—C and C—O vibrations in the polysaccharide backbone and glycerol. Finally, minor peaks in the 820–890 cm^{-1} range are due to out-of-plane C—H bending of the mannuronic and guluronic acid units in alginate (Rinaudo 2008). These spectral assignments are consistent with literature values and confirm the presence of both alginate and glycerol in the hydrogel matrix.

Comparing the hydrogel base spectra with those loaded with gallic acid, slight differences can be seen. Both spectra exhibit a broad O—H stretching band around 3200–3400 cm^{-1}, which becomes wider depending on the concentration of gallic acid suggesting enhanced hydrogen bonding due to the presence of phenolic —OH groups in the third, fourth, and fifth positions of the aromatic rings (Alfei et al. 2020; Zhang et al. 2021). An emerging band at 1683 cm^{-1} could be attributed to the C═O stretching vibration associated with the carboxylic acid that is

characteristic of gallic acid (Alfei et al. 2020). This band was more intense in the alginate-based hydrogel loaded with 0.8% gallic acid. The asymmetric stretching of carboxylate groups (COO^-) at ~1595–1610 cm^{-1} becomes slightly shifted upon gallic acid incorporation, indicating slight ionic interactions. Notably, new peaks appeared near 1515 and 1265 cm^{-1} in the loaded hydrogel, corresponding to aromatic C═C stretching and phenolic C—O vibrations, respectively, confirming the presence of gallic acid. This suggested that the biological activity of gallic acid could remain preserved even when it was integrated with the alginate-glycerol matrix. This observation was consistent with research outcomes from the literature (Gan and Chin 2021), which also found no discernible interactions between bioactive constituents and polymers, ensuring the preservation of the bioactivity of the constituents.

3.2 | Optical Characterization of Hydrogels

Apart from physicomechanical properties, other hydrogel features should be taken into account since for some applications the appearance and the color characteristics of hydrogels can be decisive. Although hydrogels based on polysaccharides are usually transparent, the addition of certain substances for their functionalization can modify optical properties (Biao et al. 2019; Dou et al. 2018). In our case, the alginate–glycerol film exhibited a transmittance of 90%, and a low opacity value, 1.7 (Table 2), being classified as a transparent material (Guzman-Puyol et al. 2022). As a consequence of the addition of gallic acid, the higher the percentage was, the less transmittance showed the functionalized hydrogel. Transmittances of 80%, 60%, and 55% were detected in the alginate hydrogels with 0.1%, 0.5%, and 0.8% of gallic acid respectively, which were significantly different among them. Contrary behavior was detected for opacity which significantly increased according to the gallic acid concentration: 2.1 in hydrogel with 0.1% of gallic acid, 2.3 in hydrogel with 0.5% of gallic acid, and 2.7 in hydrogel performed with the highest gallic acid percentage. Due to the transmittance percentage, among 10%–80%, loaded films could be classified as translucent materials (Guzman-Puyol et al. 2022). Consequently, it should be stated that the addition of gallic acid drove to hydrogels be less transparent and opaque. Similar results were observed in edible alginate hydrogels loaded with tea polyphenol extract, whose opacities increased with the increment of polyphenol content and less light was transmitted through the films (Biao et al. 2019). However, no significant differences were found in the color parameters (L^*, a^*, b^*, ΔE) in the functionalization of hydrogels with gallic acid incorporation. However, it is important to take into consideration that the use of other phenolic substances, especially phenolic extracts derived from food or plants, can substantially modify the appearance resulting in highly colored hydrogels as the extract concentration is increased (Biao et al. 2019; Dou et al. 2018).

3.3 | Functional Characterization of Hydrogels

Gallic acid with three hydroxyl groups is proven to have strong radical-scavenging activity (Sroka and Cisowski 2003). For this reason, gallic acid has been used in this study as an antioxidant agent with the aim of functionalizing sustainable macromolecular scaffolds based on alginate hydrogels.

TABLE 2 | Optical properties of alginate and gallic acid-functionalized alginate hydrogels.

Aerogels	Transmittance %	Opacity	L^*	a^*	b^*	ΔE	Photography
Alg–Gly (93:7)	90 ± 2^a	1.7 ± 0.1^a	43 ± 1^a	-0.31 ± 0.04^a	1.4 ± 0.2^a	—	
Alg–Gly (93:7), Gallic acid 0.1%	80 ± 2^b	2.1 ± 0.2^b	44 ± 3^a	-0.35 ± 0.02^a	1.6 ± 0.1^a	1.7 ± 0.4	
Alg–Gly (93:7), Gallic acid 0.5%	60 ± 2^c	2.3 ± 0.1^b	43 ± 1^a	-0.29 ± 0.01^a	1.3 ± 0.1^a	1.8 ± 0.5	
Alg–Gly (93:7), Gallic acid 0.8%	55 ± 2^d	2.7 ± 0.1^c	42 ± 1^a	-0.33 ± 0.02^a	1.5 ± 0.1^a	1.8 ± 0.3	

Note: Values with different superscripts in the same column denote significant differences among aerogels according to the Tukey post-hoc analysis ($p \leq 0.05$) when variances were homogenous, or according to T3 Dunnet post-hoc analysis ($p \leq 0.05$) for non-homogenous variances.
Abbreviations: Alg, alginate; Gly, glycerol; ΔE, color difference between alginate and gallic acid-functionalized alginate hydrogels.

The incorporation of gallic acid raised the total phenolic content of the alginate hydrogel by gradually increasing the concentration (Table 3). The strong correlation between total phenol content and antioxidant capacity has been widely claimed (Alañón et al. 2011) suggesting that polyphenols are the main contributors to antioxidant activity.

Due to a comprehensive evaluation of antioxidant capacity requires the use of several methods based on different chemistry principles, two methods with different mechanisms for inhibiting oxidation were employed. In this sense, although both chosen methods are based on a single electron transfer reaction, in the DPPH method, the $DPPH^{\cdot}$ radical is reduced by antioxidants meanwhile in the FRAP method, is a metal (Fe^{3+}) reduced into Fe^{2+} by electrons donated by antioxidants. DPPH and FRAP methods provided consistent and complementary results, as both methods confirmed that the antioxidant properties of alginate hydrogels improved with increasing gallic acid incorporation (Table 3). The addition of 0.1% of gallic acid into alginate hydrogel increased the total phenol content up to 6.0 $mg_{gallic\ acid}/g_{hydrogel}$ which implied an antioxidant activity of 6.6 $mg_{gallic\ acid}/g_{hydrogel}$ and 0.19 $mmol_{FeSO4}/g_{hydrogel}$ according to DPPH and FRAP methods, respectively. Antioxidant values were increased about 4.8 and 4.4-fold with the addition of 0.5% of gallic acid into alginate hydrogels. These values were greatly improved when the maximum concentration of gallic acid tested was incorporated. The ability to scavenge free radicals of hydrogels loaded with 0.8% of gallic acid was enhanced around 7.0-fold and 7.3-fold in DPPH and FRAP methods, respectively, compared with those hydrogels loaded with the minimum percentage of gallic acid tested, reaching values of 46.0 $mg_{gallic\ acid}/g_{hydrogel}$ and 1.40 $mmol_{FeSO4}/g_{hydrogel}$. Although several studies have confirmed the increase of antioxidant properties of films by adding polyphenols, differences in measurements of antioxidant activity determined by non-standardized methods with different protocols and ways to express the results make the comparison difficult with those reported in the literature. The addition of 5.0% of tea polyphenol extract to sodium alginate films increased antioxidant activity by about 7.1-fold according to the DPPH method and 41.0-fold when the ABTS assay was used (Biao et al. 2019). Previously, lower percentages of tea polyphenols (0.4%–2.0%) were also loaded into gelatin sodium alginate films exhibiting an increase of antioxidant activity around 2.52-fold (DPPH) and 1.54-fold (ABTS) (Dou et al. 2018). Therefore, it seems that a lower percentage of gallic acid is required to functionalize hydrogels compared with the polyphenol extract doses used for the same purposes.

In addition, the release of gallic acid from functionalized hydrogels in phosphate-buffer saline for 24 h at 37°C was monitored (Figure 4).

The release of gallic acid from the hydrogels exhibited a dose-dependent behavior; higher concentrations of gallic acid in the formulation resulted in greater amounts being released. Interestingly, despite differences in loading, all hydrogels showed a similar release profile characterized by an initial burst—reaching peak release within the first one to two hours—followed by a gradual decline. This decline in gallic acid concentration over time may be attributed to interactions with sodium salts in the release medium, leading to the formation of gallic acid salts such

TABLE 3 | Total phenol content (TPC) and antioxidant activity measured by DPPH and FRAP methods of gallic acid-functionalized alginate hydrogels.

Hydrogles	Total phenol content	Antioxidant activity	
	TPC ($mg_{gallic\ acid}/g_{aerogel}$)	DPPH ($mg_{gallic\ acid}/g_{aerogel}$)	FRAP ($mmol_{FeSO4}/g_{aerogel}$)
Alg–Gly (93:7)	—	—	—
Alg–Gly (93:7), Gallic acid 0.1%	6.0 ± 0.4^{c}	6.6 ± 0.5^{c}	0.19 ± 0.01^{c}
Alg–Gly (93:7), Gallic acid 0.5%	23 ± 1^{b}	32 ± 2^{b}	0.84 ± 0.04^{b}
Alg–Gly (93:7), Gallic acid 0.8%	45.1 ± 0.3^{a}	46 ± 3^{a}	1.4 ± 0.1^{a}

Note: Values with different superscripts in the same column denote significant differences among aerogels according to the Tukey's post-hoc analysis ($p \leq 0.05$) when variances were homogenous, or according to T3 Dunnet post-hoc analysis ($p \leq 0.05$) for non-homogenous variances.
Abbreviations: Alg, alginate; Gly, glycerol.

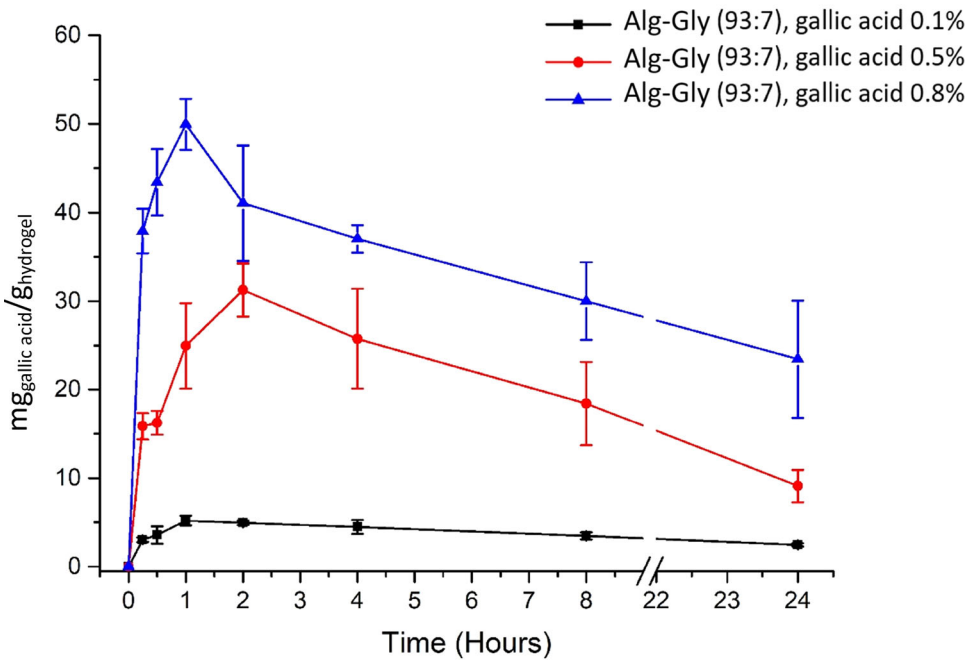

FIGURE 4 | Release of gallic acid from functionalized hydrogels in phosphate-buffer saline for 24 h by means of antioxidant activity measurement based on DPPH method.

as sodium gallate, which possesses reduced antioxidant activity (Cláudio et al. 2012). Consequently, the antioxidant activity also decreases after the initial release peak. For this reason, the antioxidant activity decreases with time after the maximum release peak (1–2 h). Although long-term migration studies on real foods are necessary, these results indicate that the gallic acid content is released within 1–2 h in aqueous media, making it useful for the protection of highly perishable or oxidized foods such as fresh or cut fruits and vegetables.

4 | Conclusions

Gallic acid-enhanced alginate hydrogels offer a sustainable and distinctive material to be used as a plastic replacement in food packaging. The addition of gallic acid improved the mechanical and functional properties, representing a significant advancement in the field of sustainable biomaterials. In general terms, thickness, opacity, WVP, and swelling degree increased as a consequence of gallic acid incorporation. The functionalization also made the hydrogels less resistant to tensile forces and crack propagation due to increased porosity—particularly at the highest tested concentration (0.8%)—though elasticity remained unaffected. Notably, the incorporation of gallic acid led to a 7.0–7.3-fold increase in antioxidant activity at higher concentrations. Understanding these underlying structural, mechanical, and functional changes provides valuable insight for customizing hydrogels with tailored properties, enhancing their effectiveness for specific applications. This diversity of findings helps to develop a more nuanced perspective on the multifaceted impacts of gallic acid in functionalized alginate hydrogels, enabling more informed design strategies. In view of the results obtained, these materials may have potential use as packaging for whole or cut fresh foods with a considerable water content (strawberries, apples, and avocados), as their low swelling, low water vapor permeability, antioxidant capacity together with their mechanical properties offer the necessary properties to prolong the shelf life of this type of food.

Acknowledgments

Authors are grateful for project 2023-GRIN-34333, Programa FEDER Castilla-La Mancha and the project I+D+i PID2021-125188OA-C33 funded by MICIU/AEI/10.13039/501100011033, by ERDF, EU, A way of making Europe. F.J.L.J. thanks to the grant FJC2020-044298-I funded by MCIN/AEI/10.13039/501100011033 and by European Union NextGeneration EU/PRTR.

Conflicts of Interest

The authors declare no conflicts of interest.

Data Availability Statement

The data that support the findings of this study are available from the corresponding author upon reasonable request.

References

Solbu, A. A., A. Koernig, J. S. Kjesbu, D. Zaytseva-Zotova, M. Sletmoen, and B. L. Strand. 2022. "High Resolution Imaging of Soft Alginate Hydrogels by Atomic Force Microscopy." *Carbohydrate Polymers* 276: 118804. https://doi.org/10.1016/j.carbpol.2021.118804.

Alañón, M. E., L. Castro-Vázquez, M. C. Díaz-Maroto, I. Hermosín-Gutiérrez, M. H. Gordon, and M. S. Pérez-Coello. 2011. "Antioxidant Capacity and Phenolic Composition of Different Woods Used in Cooperage." *Food Chemistry* 129, no. 4: 1584–1590. https://doi.org/10.1016/j.foodchem.2011.06.013.

Alfei, S., B. Marengo, and C. Domenicotti. 2020. "Development of a Fast, Low-Cost, Conservative and Ecological Method for Quantifying Gallic Acid in Polymeric Formulations by FTIR Spectroscopy in Solu-

tion." *ChemistrySelect* 5, no. 14: 4381–4388. https://doi.org/10.1002/slct.202000690.

ASTM Commitee. 2016. "Standard Test Methods for Water Vapor Transmission of Materials (E96/E96M-16)." In Annual Book of ASTM Standards, edited by A. International. https://doi.org/10.1520/E0096_E0096M-16.

Barboza-Carmona, J. D., M. Wenzel, L. Eckert, D. Enke, J. Matysik, and I. F. Céspedes-Camacho. 2022. "A Spectroscopic Insight of the Porous Structure of Hydrophobic Silica Aerogels by Hyperpolarized 129Xe NMR." *Journal of Sol-Gel Science and Technology* 101, no. 1: 176–184. https://doi.org/10.1007/s10971-021-05684-x.

Batista, R. A., P. J. P. Espitia, J. Quintans, et al. 2019. "Hydrogel as an Alternative Structure for Food Packaging Systems." *Carbohydrate Polymers* 205: 106–116. https://doi.org/10.1016/j.carbpol.2018.10.006.

Bento, C. S. A., S. Alarico, N. Empadinhas, H. C. de Sousa, and M. E. M. Braga. 2022. "Sequential scCO2 Drying and Sterilisation of Alginate-Gelatine Aerogels for Biomedical Applications." *Journal of Supercritical Fluids* 184: 105570. https://doi.org/10.1016/j.supflu.2022.105570.

Benzie, I. F. F., and J. J. Strain. 1996. "The Ferric Reducing Ability of Plasma (FRAP) as a Measure of 'Antioxidant Power': The FRAP Assay." *Analytical Biochemistry* 239, no. 1: 70–76. https://doi.org/10.1006/abio.1996.0292.

Biao, Y., C. Yuxuan, T. Qi, et al. 2019. "Enhanced Performance and Functionality of Active Edible Films by Incorporating Tea Polyphenols Into Thin Calcium Alginate Hydrogels." *Food Hydrocolloids* 97: 105197. https://doi.org/10.1016/j.foodhyd.2019.105197.

Carbone, K., V. Macchioni, G. Petrella, D. O. Cicero, and L. Micheli. 2021. "Humulus Lupulus Cone Extract Efficacy in Alginate-Based Edible Coatings on the Quality and Nutraceutical Traits of Fresh-Cut Kiwifruit." *Antioxidants* 10, no. 9: 1395. https://doi.org/10.3390/antiox10091395.

Chen, Z., P. Li, Q. Ji, Y. Xing, X. Ma, and Y. Xia. 2023. "All-Polysaccharide Composite Films Based on Calcium Alginate Reinforced Synergistically by Multidimensional Cellulose and Hemicellulose Fractionated From Corn Husks." *Materials Today Communications* 34: 105090. https://doi.org/10.1016/j.mtcomm.2022.105090.

Choi, I., Y. Lee, J. S. Lyu, J.-S. Lee, and J. Han. 2022. "Characterization of Ionically Crosslinked Alginate Films: Effect of Different Anion-Based Metal Cations on the Improvement of Water-Resistant Properties." *Food Hydrocolloids* 131: 107785. https://doi.org/10.1016/j.foodhyd.2022.107785.

Cláudio, A. F. M., A. M. Ferreira, C. S. R. Freire, A. J. D. Silvestre, M. G. Freire, and J. A. P. Coutinho. 2012. "Optimization of the Gallic Acid Extraction Using Ionic-Liquid-Based Aqueous Two-Phase Systems." *Separation and Purification Technology* 97: 142–149. https://doi.org/10.1016/j.seppur.2012.02.036.

Coldebella, R., M. Gentil, C. Berger, et al. 2021. "Nanofibrillated Cellulose-Based Aerogels Functionalized With Tajuva (*Maclura tinctoria*) Heartwood Extract." *Polymers* 13, no. 6: 908. https://doi.org/10.3390/polym13060908.

Dou, L., B. Li, K. Zhang, X. Chu, and H. Hou. 2018. "Physical Properties and Antioxidant Activity of Gelatin-Sodium Alginate Edible Films With Tea Polyphenols." *International Journal of Biological Macromolecules* 118: 1377–1383. https://doi.org/10.1016/j.ijbiomac.2018.06.121.

Dufour, T. 2023. "From Basics to Frontiers: A Comprehensive Review of Plasma-Modified and Plasma-Synthesized Polymer Films." *Polymers* 15, no. 17: 3607. https://doi.org/10.3390/polym15173607.

Essifi, K., A. Ed-Daoui, D. Berraaouan, M. Benelmostafa, M. Dahmani, and A. Tahani. 2020. "Determination of the Mechanical Properties of Single Calcium Alginate Microbeads Loaded Gallic Acid." *Materials Today: Proceedings* 31: S45–S50. https://doi.org/10.1016/j.matpr.2020.05.747.

European Commission. 2020. Circular Economy Action Plan. Directorate-General for Environment, European Commission. Adopted 11 March 2020. https://op.europa.eu/en/publication-detail/-/publication/9dc6aa01-39d2-11eb-b27b-01aa75ed71a1/language-en.

Fabra, M. J., I. Falcó, W. Randazzo, G. Sánchez, and A. López-Rubio. 2018. "Antiviral and Antioxidant Properties of Active Alginate Edible Films Containing Phenolic Extracts." *Food Hydrocolloids* 81: 96–103. https://doi.org/10.1016/j.foodhyd.2018.02.026.

Feng, W., L. Li, C. Yang, A. Welle, O. Trapp, and P. A. Levkin. 2015. "UV-Induced Tetrazole-Thiol Reaction for Polymer Conjugation and Surface Functionalization." *Angewandte Chemie International Edition* 54, no. 30: 8732–8735. https://doi.org/10.1002/anie.201502954.

Fernández-Ponce, M. T., E. Gómez, C. Cejudo-Bastante, et al. 2021. "Development of Functionalized Alginate Dressing With Mango Polyphenols by Supercritical Technique to be Employed as an Antidiabetic Transdermal System." *Journal of Supercritical Fluids* 175: 105274. https://doi.org/10.1016/j.supflu.2021.105274.

Firoznezhad, M., R. Abi-Rached, F. Fulgheri, et al. 2023. "Design and in Vitro Effectiveness Evaluation of Echium Amoenum Extract Loaded in Bioadhesive Phospholipid Vesicles Tailored for Mucosal Delivery." *International Journal of Pharmaceutics* 634: 122650. https://doi.org/10.1016/j.ijpharm.2023.122650.

Gan, J.-E., and C.-Y. Chin. 2021. "Formulation and Characterisation of Alginate Hydrocolloid Film Dressing Loaded With Gallic Acid for Potential Chronic Wound Healing." *F1000Research* 10: 451. https://doi.org/10.12688/f1000research.52528.1.

Giz, A. S., M. Berberoglu, S. Bener, et al. 2020. "A Detailed Investigation of the Effect of Calcium Crosslinking and Glycerol Plasticizing on the Physical Properties of Alginate Films." *International Journal of Biological Macromolecules* 148: 49–55. https://doi.org/10.1016/j.ijbiomac.2020.01.103.

Gorshkova, N., O. Brovko, I. Palamarchuk, K. Bogolitsyn, and A. Ivakhnov. 2021. "Preparation of Bioactive Aerogel Material Based on Sodium Alginate and Chitosan for Controlled Release of Levomycetin." *Polymers for Advanced Technologies* 32, no. 9: 3474–3482. https://doi.org/10.1002/pat.5358.

Guan, F., J. Tao, Q. Yao, et al. 2024. "Alginate-Based Aerogel Fibers With a Sheath-Core Structure for Highly Efficient Methylene Blue Adsorption via Directed Freezing Wet-Spinning." *Colloids and Surfaces A: Physicochemical and Engineering Aspects* 680: 132706. https://doi.org/10.1016/j.colsurfa.2023.132706.

Guzman-Puyol, S., J. J. Benítez, and J. A. Heredia-Guerrero. 2022. "Transparency of Polymeric Food Packaging Materials." *Food Research International* 161: 111792. https://doi.org/10.1016/j.foodres.2022.111792.

Harlen, W. C., S. Prakash, S. Yuliani, and B. Bhandari. 2025. "Encapsulation of Gallic Acid in Alginate/Lactoferrin Composite Hydrogels: Physical Properties and Gallic Acid Diffusion." *Food Hydrocolloids* 160: 110784. https://doi.org/10.1016/j.foodhyd.2024.110784.

ISO 37. 2024. ISO 37:2017. Rubber, vulcanized or thermoplastic — Determination of tensile stress-strain properties.

Jejurikar, A., X. T. Seow, G. Lawrie, D. Martin, A. Jayakrishnan, and L. Grøndahl. 2012. "Degradable Alginate Hydrogels Crosslinked by the Macromolecular Crosslinker Alginate Dialdehyde." *Journal of Materials Chemistry* 22, no. 19: 9751. https://doi.org/10.1039/c2jm30564j.

Leyva-Jiménez, F. J., R. Oliver-Simancas, I. Castangia, A. M. Rodríguez-García, and M. E. Alañón. 2023. "Comprehensive Review of Natural Based Hydrogels as an Upcoming Trend for Food Packing." *Food Hydrocolloids* 135: 108124. https://doi.org/10.1016/j.foodhyd.2022.108124.

Li, J., S. Y. Kim, X. Chen, and H. J. Park. 2016. "Calcium-Alginate Beads Loaded With Gallic Acid: Preparation and Characterization." *LWT—Food Science and Technology* 68: 667–673. https://doi.org/10.1016/j.lwt.2016.01.012.

Li, X.-L., M.-J. Chen, and H.-B. Chen. 2019. "Facile Fabrication of Mechanically-Strong and Flame Retardant Alginate/Clay Aerogels." *Composites Part B: Engineering* 164: 18–25. https://doi.org/10.1016/j.compositesb.2018.11.055.

Liu, G., Z. Ding, Q. Yuan, H. Xie, and Z. Gu. 2018. "Multi-Layered Hydrogels for Biomedical Applications." *Frontiers in Chemistry* 6: 439. https://doi.org/10.3389/fchem.2018.00439.

Liu, Y., C.-J. Zhang, J.-C. Zhao, Y. Guo, P. Zhu, and D.-Y. Wang. 2016. "Bio-Based Barium Alginate Film: Preparation, Flame Retardancy and Thermal Degradation Behavior." *Carbohydrate Polymers* 139: 106–114. https://doi.org/10.1016/j.carbpol.2015.12.044.

Lovskaya, D. D., A. E. Lebedev, and N. V. Menshutina. 2015. "Aerogels as Drug Delivery Systems: In Vitro and in Vivo Evaluations." *Journal of Supercritical Fluids* 106: 115–121. https://doi.org/10.1016/j.supflu.2015.07.011.

Manzocco, L., K. S. Mikkonen, and C. A. García-González. 2021. "Aerogels as Porous Structures for Food Applications: Smart Ingredients and Novel Packaging Materials." *Food Structure* 28: 100188. https://doi.org/10.1016/j.foostr.2021.100188.

Martins, M., A. A. Barros, S. Quraishi, et al. 2015. "Preparation of Macroporous Alginate-Based Aerogels for Biomedical Applications." *Journal of Supercritical Fluids* 106: 152–159. https://doi.org/10.1016/j.supflu.2015.05.010.

Nešić, A., M. Gordić, S. Davidović, et al. 2018. "Pectin-Based Nanocomposite Aerogels for Potential Insulated Food Packaging Application." *Carbohydrate Polymers* 195: 128–135. https://doi.org/10.1016/j.carbpol.2018.04.076.

Niknia, N., R. Kadkhodaee, and M. N. Eshtiaghi. 2020. "Gum Tragacanth-Polyvinyl Alcohol Aerogel for Oral Delivery of Silymarin." *International Journal of Biological Macromolecules* 157: 151–157. https://doi.org/10.1016/j.ijbiomac.2020.04.202.

Pawar, S. N., and K. J. Edgar. 2012. "Alginate Derivatization: A Review of Chemistry, Properties and Applications." *Biomaterials* 33, no. 11: 3279–3305. https://doi.org/10.1016/j.biomaterials.2012.01.007.

Pereira, R., A. Mendes, and P. Bártolo. 2013. "Alginate/Aloe Vera Hydrogel Films for Biomedical Applications." *Procedia CIRP* 5: 210–215. https://doi.org/10.1016/j.procir.2013.01.042.

Rinaudo, M. 2008. "Main Properties and Current Applications of Some Polysaccharides as Biomaterials." *Polymer International* 57, no. 3: 397–430. https://doi.org/10.1002/pi.2378.

Russo, R., M. Malinconico, and G. Santagata. 2007. "Effect of Cross-Linking With Calcium Ions on the Physical Properties of Alginate Films." *Biomacromolecules* 8, no. 10: 3193–3197. https://doi.org/10.1021/bm700565h.

dos Santos, P., J. Viganó, G. Furtado, et al. 2020. "Production of Resveratrol Loaded Alginate Aerogel: Characterization, Mathematical Modeling, and Study of Impregnation." *Journal of Supercritical Fluids* 163: 104882. https://doi.org/10.1016/j.supflu.2020.104882.

Selvasekaran, P., and R. Chidambaram. 2021. "Food-Grade Aerogels Obtained From Polysaccharides, Proteins, and Seed Mucilages: Role as a Carrier Matrix of Functional Food Ingredients." *Trends in Food Science & Technology* 112: 455–470. https://doi.org/10.1016/j.tifs.2021.04.021.

Sharma, M., K. K. Dash, and L. S. Badwaik. 2022. "Physicochemical and Release Behaviour of Phytochemical Compounds Based on Black Jamun Pulp Extracts-Filled Alginate Hydrogel Beads Through Vibration Dripping Extrusion." *International Journal of Biological Macromolecules* 194: 715–725. https://doi.org/10.1016/j.ijbiomac.2021.11.116.

Shivakumara, L. R., and T. Demappa. 2019. "Synthesis and Swelling Behaviour of Sodium Alginate/Poly(Vinyl Alcohol) Hydrogels." *Turkish Journal of Pharmaceutical Sciences* 16: 252–260. https://doi.org/10.4274/tjps.galenos-2018.92408.

Siddiqui, S. A., S. Khan, M. Mehdizadeh, et al. 2023. "Phytochemicals and Bioactive Constituents in Food Packaging—A Systematic Review." *Heliyon* 9, no. 11: e21196. https://doi.org/10.1016/j.heliyon.2023.e21196.

Smirnova, I., and P. Gurikov. 2018. "Aerogel Production: Current Status, Research Directions, and Future Opportunities." *Journal of Supercritical Fluids* 134: 228–233. https://doi.org/10.1016/j.supflu.2017.12.037.

Sroka, Z., and W. Cisowski. 2003. "Hydrogen Peroxide Scavenging, Antioxidant and Anti-Radical Activity of Some Phenolic Acids." *Food and Chemical Toxicology* 41, no. 6: 753–758. https://doi.org/10.1016/S0278-6915(02)00329-0.

Sun, G., T. Liang, W. Tan, and L. Wang. 2018. "Rheological Behaviors and Physical Properties of Plasticized Hydrogel Films Developed From κ-carrageenan Incorporating Hydroxypropyl Methylcellulose." *Food Hydrocolloids* 85: 61–68. https://doi.org/10.1016/j.foodhyd.2018.07.002.

Vidal, A., A. Giacaman, S. S. Orellana, et al. 2020. "Application of Chitosan and Chondroitin Sulphate Aerogels in a Patient with Diabetes with an Open Forefoot Transmetatarsal Amputation." *Wounds: A Compendium of Clinical Research and Practice* 32, no. 3: E14–E18. http://www.ncbi.nlm.nih.gov/pubmed/32335521.

Viganó, J., A. A. D. Meirelles, G. Náthia-Neves, et al. 2020. "Impregnation of Passion Fruit Bagasse Extract in Alginate Aerogel Microparticles." *International Journal of Biological Macromolecules* 155: 1060–1068. https://doi.org/10.1016/j.ijbiomac.2019.11.070.

Yan, P., W. Lan, and J. Xie. 2025. "Characterizations of Two Physically Modified Sodium Alginate Composite Films Doped With Gallic Acid and Their Preservation of Refrigerated Sea Bass (*Lateolabrax maculatus*)." *Food Chemistry* 474: 143147. https://doi.org/10.1016/j.foodchem.2025.143147.

Ye, Z., H. Lu, G. Chai, C. Wu, J. Chen, and L. Lv. 2023. "Glycerol-Modified Poly(Vinyl Alcohol)/Poly(Ethylene Glycol) Self-Healing Hydrogel for Artificial Cartilage." *Polymer International* 72, no. 1: 27–38. https://doi.org/10.1002/pi.6444.

Zhan, M., M. Guo, Y. Jiang, and X. Wang. 2015. "Characterization of the Interaction Between Gallic Acid and Lysozyme by Molecular Dynamics Simulation and Optical Spectroscopy." *International Journal of Molecular Sciences* 16, no. 12: 14786–14807. https://doi.org/10.3390/ijms160714786.

Zhang, A., Y. Zou, Y. Xi, et al. 2021. "Fabrication and Characterization of Bamboo Shoot Cellulose/Sodium Alginate Composite Aerogels for Sustained Release of Curcumin." *International Journal of Biological Macromolecules* 192: 904–912. https://doi.org/10.1016/j.ijbiomac.2021.10.027.

Zhou, W., J. Fang, S. Tang, Z. Wu, and X. Wang. 2021. "3D-Printed Nanocellulose-Based Cushioning—Antibacterial Dual-Function Food Packaging Aerogel." *Molecules* 26, no. 12: 3543. https://doi.org/10.3390/molecules26123543.